

Article

Investigation of Following Vehicles' Driving Patterns Using Spectral Analysis Techniques

Chandle Chae ¹  and Youngho Kim ^{2,*}

¹ Division for Road Transport Policy, Korea Transport Institute, Sejong-si 30147, Republic of Korea; culfield@koti.re.kr

² Department of Mobility Transformation Research, Korea Transport Institute, Sejong-si 30147, Republic of Korea

* Correspondence: ykim@koti.re.kr; Tel.: +82-44-211-3131

Abstract: Despite the potential benefits of autonomous vehicles (AVs) of reducing human driver errors and enhancing traffic safety, a comprehensive evaluation of recent AV collision data reveals a concerning trend of rear-end collisions caused by following vehicles. This study aimed to address this issue by developing a methodology that identifies the relationship between driving patterns and the risk of collision between leading and following vehicles using spectral analysis. Specifically, we propose a process for computing three indices: reaction time, stimulus compliance index, and collision-risk aversion index. These indices consistently produced reliable results under various traffic conditions. Our findings align with existing research on the driving patterns of following vehicles. Given the consistency and robustness of these indices, they can be effectively utilized in advanced driver assistance systems or incorporated into AVs to assess the likelihood of collision risk posed by following vehicles and develop safer driving strategies accordingly.

Keywords: sustainable traffic management; autonomous vehicle; driving behavior; car following; spectral analysis



check for updates

Citation: Chae, C.; Kim, Y. Investigation of Following Vehicles' Driving Patterns Using Spectral Analysis Techniques. *Sustainability* **2023**, *15*, 10539. <https://doi.org/10.3390/su151310539>

Academic Editors: Junyoung Park, Yina Wu, Hochul Park and Bin Ji

Received: 1 June 2023

Revised: 29 June 2023

Accepted: 3 July 2023

Published: 4 July 2023



Copyright: © 2023 by the authors. Licensee MDPI, Basel, Switzerland. This article is an open access article distributed under the terms and conditions of the Creative Commons Attribution (CC BY) license (<https://creativecommons.org/licenses/by/4.0/>).

1. Introduction

According to the National Highway Traffic Safety Administration (NHTSA), rear-end collision is the most frequent type of crash among motorized users [1]. Almost 30% of all car accidents in the U.S. are rear-end collisions, with nearly 2.5 million being reported every year. These collisions typically occur when the preceding car suddenly decelerates or when the following car accelerates more rapidly than the preceding car. Drivers' inattention, unintentional close following due to misjudgment of the required deceleration, and deliberate aggressive close following are the main factors contributing to rear-end collisions [2]. Significant research has been conducted to improve drivers' ability to prevent such accidents by integrating collision warning systems or advanced driver assistance systems (ADASs) onboard vehicles [3,4].

Autonomous vehicles (AVs) are expected to cause a paradigm shift in road traffic safety. However, according to Tesla's annual report, about 830,000 vehicles have been sold in the United States since 2015, when vehicles equipped with the Autopilot function began to be sold, and a total of 35 traffic accidents have occurred. Despite the potential of AVs to eliminate human driver errors and enhance traffic safety, a comprehensive evaluation of recent AV collision data indicates that modern AVs are prone to rear-end collisions with following vehicles.

Generally, it is unrealistic to expect all conventional vehicles (CVs) to be converted into AVs within a few days. If the transition from a fleet of CVs to a fleet of AVs occurs over a long period, AVs must make proper decisions in safety-critical situations by interacting with the surrounding CVs for sustainable traffic management. Accidents involving AVs often occur because of their failure to respond reasonably to the behaviors of surrounding

CVs. Therefore, a firm understanding of the collision risk posed by CVs is essential for AVs to make safe driving decisions.

The collision risk in a certain traffic situation is calculated using safety surrogate measures (SSMs), which rely on microscopic traffic variables such as an individual vehicle's speed, acceleration, time headway, and space headway [5]. However, most SSMs are highly dependent on mathematical models based on physical dynamics, which can limit their accuracy because they estimate collision risk based on the assumption of constant vehicle velocity. Additionally, these measures do not consider the driving-pattern data collected from vehicles. To reduce the occurrence of rear-end collisions, it is crucial to continuously analyze the driving behaviors of surrounding vehicles and activate preventive or protective measures accordingly. The aim of this study was to develop a new methodology for identifying the driving patterns of following vehicles based on data collected in car-following situations in an observation interval. By identifying the driving patterns of following vehicles, effective measures can be developed for AVs to prevent rear-end collisions with following vehicles.

The remainder of this paper is organized as follows: First, a brief review of the existing literature on the assessment of collision risk is presented. We then propose a process for driving-pattern assessment and introduce driving-pattern indices for following vehicles. The results of the driving-pattern indices are discussed in detail. Finally, the study concludes with a summary of its main findings and implications.

2. Literature Review

There are several ways to abstract and model real traffic events depending on the level of aggregation. Macroscopic traffic flow models describe collective vehicle dynamics in terms of aggregate traffic variables such as density, flow, and speed using fluid dynamics models [6]. Microscopic traffic flow models, on the other hand, describe the dynamics of individual vehicles and their interactions using car-following models and cellular automata models [7,8]. Mesoscopic traffic flow models describe microscopic vehicle dynamics as functions of macroscopic fields using gas kinetics models [9]. Among the three modeling approaches, microscopic traffic flow models are becoming increasingly important owing to the widespread use of ADASs, such as adaptive cruise control (ACC), infrastructure-to-vehicle (I2V) and vehicle-to-vehicle (V2V) communications, and other applications of intelligent transport systems (ITSs). Additionally, the deployment of AVs in smart mobility services is becoming increasingly common worldwide [10].

Microscopic models are used to describe the behavior of individual vehicles with three primary actions: acceleration, deceleration, and steering. The collective behavior of individual vehicles results in a macroscopic traffic flow. Microscopic models can be classified into two categories: car-following and lane-changing models. Car-following models describe the longitudinal dynamics of individual vehicles, such as acceleration and deceleration, based on the movement of the preceding vehicle in the same lane. On the other hand, lane-changing models do not include the steering-induced lateral dynamics of individual vehicles but rather describe lane-changing decisions and related actions. It is assumed that the lane-changing maneuver occurs instantaneously. Therefore, the present study, which proposes an assessment methodology for driving patterns and rear-end collision risk in certain time intervals, does not consider lane-changing behaviors.

The first car-following models were proposed in the 1950s by Reuschel [11] and Pipes [12]. Since then, many variants have been developed. The Gazis–Herman–Rothery (GHR) model explains the relationship between two vehicles based on stimuli, response, and sensitivity [13]. The model captures many essential features at the qualitative level and provides a framework for mathematical stability analysis. However, it cannot properly describe the traffic phenomena in the free-flow state. Gipps developed a behavioral car-following model in which a driver alters his/her speed to reach the desired speed or safely follows the leader [14]. Measurement models have been proposed to explain the desire of a driver to maintain the minimum space headway [15]. Existing car-following

models have been developed under the assumption that two vehicles must adhere to one of the minimum safety requirements, such as minimum safety distance, minimum reaction time, and minimum deceleration rate. Recently, research on a car-following model that reflects the driving behavior of an automated vehicle has been conducted. Y. Zhou et al. developed a methodology to adjust the car-following behavior of connected and automated vehicles (CAVs) using V2X communication [16], and W. Kontar et al. developed a model to predict car-following behaviors of AVs. They proposed a logistic classifier coupled with a convoluted multivariate Gaussian process (MGP) [17]. However, these models have the limitation that they cannot describe risky situations that do not follow the basic assumption of the minimum safety requirements. To develop ADASs and AVs that can operate correctly in real traffic situations, a robust tool to describe rare events, such as near-collision and collision events, is needed. Yajie Zou et al. developed a coupled hidden Markov model (CHMM) that can explain the intra-heterogeneity of individual drivers [18], and Jon Ander Ruiz Colmenares et al. conducted research to derive driving behavior that causes motion sickness using machine learning techniques [19]. Yuchuan Du et al. developed a deep reinforcement learning technique that enables autonomous vehicles to perform comfortable and energy-efficient speed control on rough pavement [20]. SSMs are crucial to representing the contributing factors and failure mechanisms that lead to road collisions because it is challenging to collect data on such rare events. Although historical collision data are available, they do not include near-collision data, which are also critical to improving safety. Several SSMs have been developed to estimate collision risk in car-following situations, including the time-to-collision (TTC) method developed by Hayward [21], which estimates the risk of collision between two consecutive vehicles. However, TTC has limitations in representing the collision risk under various traffic conditions. Modified TTC methods have been proposed, and stopping distance-based SSMs, such as the stopping distance index (SDI), stopping headway distance (SHD), and the crash index (CI), have high sensitivity but still do not fully reflect human reaction behavior [22].

As a result of the literature review, driving behavior models only explain overall behavior but have limitations in that they cannot explain the risky driving behavior required by AVs for decision making. On the other hand, collision-risk models, including SSMs, cannot identify potential risky driving tendencies because they calculate risk according to the relationship between two vehicles at a specific point in time. Therefore, a methodology that can identify the potential risky driving tendency of a following vehicle is needed by AVs for safe decision making. This risky driving tendency can be derived from the response change of the following vehicle according to the stimulus of the leading vehicle, and this study proposes a methodology to analyze the relative speed wave appearing as the response of the following vehicle using spectral analysis.

Spectral analysis is used to transform temporal variance information into frequency variance information, thereby providing insights into the periodicity and dominant frequencies of a time series. Abdüsselam Altunkaynak et al. predicted hourly significant wave height using spectral analysis-based models [23], and Wuan Wang et al. applied spectral analysis to identify drivers' behaviors before and after the start of distracted driving [24]. This technique has also been applied to the field of traffic analysis, where it can reveal information regarding the distribution characteristics of the frequency components and provide valuable information for developing traffic forecasting models.

The objective of this research was to use spectral analysis to identify driving behavior and collision risk among vehicles in mixed traffic streams, including both autonomous and human-driven vehicles. By identifying the dominant frequencies in the data, we hope to better understand the relationship between driving behavior and collision risk and to develop more effective methods to prevent rear-end collisions and improve traffic safety.

3. Methodology

The relative speed data of preceding and following vehicles over a certain period conform to a waveform, as shown in Figure 1.

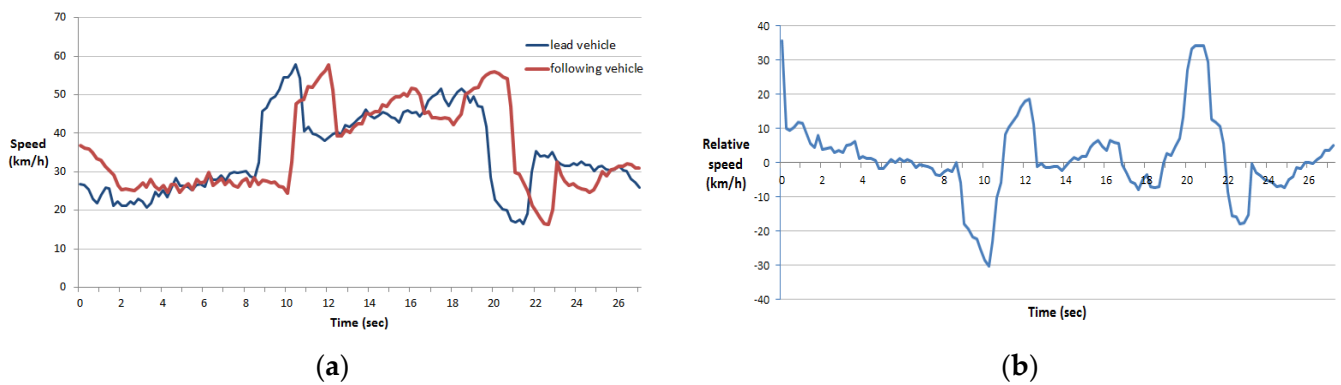


Figure 1. Waveforms in car following: (a) speed data and (b) relative speed.

The waveforms show a periodic behavior resulting from the stimulus provided by the preceding vehicle and the reaction of the following vehicle. They demonstrate various types of fluctuations and frequencies depending on the scale of the following vehicle’s reaction to the preceding vehicle’s acceleration and deceleration. Consequently, wave analysis can provide valuable insights into the driving behavior of a following vehicle. This section presents a useful methodology that employs the spectral analysis of vehicle trajectory data collected in car-following situations to elucidate the driving patterns of following vehicles.

The trajectories of individual vehicles were obtained using image detectors installed along a 600 m section of the Seoul Ring Expressway, at temporal resolution of 0.2 s, from 13 May to 26 May 2010. Despite the 13-year gap since the data collection period, the findings of this study are applied with the assumption that driver behavior is closely linked to human nature and is not expected to change significantly over time. To ensure the suitability of the dataset for analysis, the minimum observation time required to capture the reaction characteristics of following vehicles was set to 10 s. A total of 170 datasets containing car-following behaviors of more than 10 s were used in this study. The power spectrum density (PSD) was computed from 170 relative speed datasets using MATLAB. The process of evaluating the driving pattern of the following vehicle consisted of four steps, ① modification of TTC, ② calculation of PSD, ③ correlation analysis between the modified TTC and PSD, and ④ development of driving-pattern indices, as shown in Figure 2.

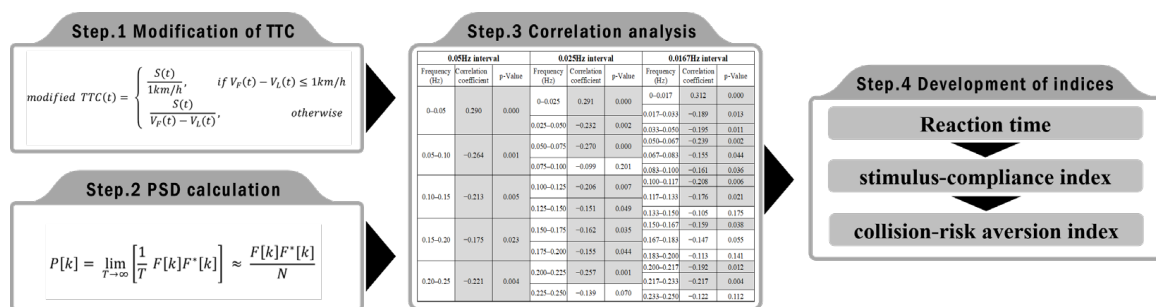


Figure 2. Driving-pattern assessment flow chart.

With this process, three driving-pattern indices that can analyze the risky driving behavior of following vehicles in a car-following relationship were developed, i.e., reaction time, stimulus compliance index, and collision-risk aversion index, as shown in Figure 3. Reaction time is the time taken for the following vehicle to respond to the leading vehicle’s stimulus, and the stimulus compliance index is the correlation between the size of the stimuli of the leading vehicle and the following vehicle. The stimulus compliance index is calculated as a value between -1 and 1 , and the closer to 1 it is, the greater the positive correlation is. The following section provides detailed descriptions of these indices.

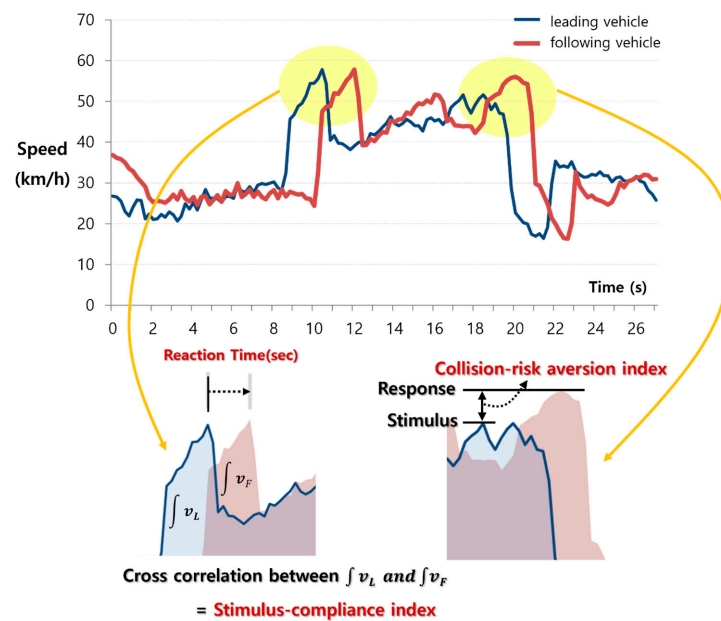


Figure 3. Driving-pattern indices.

4. Driving-Pattern Assessment of Following Vehicles

4.1. Step 1: Modification of TTC

TTC is the conventional metric for assessing the risk of rear-end collision between two vehicles in a car-following situation. TTC is defined as the time remaining until a collision occurs between two vehicles based on the assumption that both vehicles maintain their current speed in a car-following situation [12]. TTC can be calculated using Equation (1), where $V_L(t)$ represents the speed of the preceding vehicle at time t , $V_F(t)$ represents the speed of the following vehicle at time t , and $S(t)$ represents the distance between the two vehicles at time t .

$$TTC = \frac{S(t)}{V_F(t) - V_L(t)} \quad (1)$$

To evaluate a new method for assessing the collision risk of a following vehicle, a robust risk assessment metric is required as a reference index. However, TTC cannot be compared with relative speed data owing to the following limitations: When $V_F(t) < V_L(t)$, TTC yields a negative value, rendering the assessment of risk impossible. If the relative speed between the two vehicles is very low (below 1 km/h), TTC is overestimated and approaches infinity. In congested traffic, the potential collision risk increases as the distance between the two vehicles, $S(t)$, decreases. However, TTC yields a large value because the relative speed also decreases with congestion. Therefore, this study proposes a modification of TTC in Equation (2) to overcome these limitations.

$$\text{modified } TTC(t) = \begin{cases} \frac{S(t)}{1 \text{ km/h}}, & \text{if } V_F(t) - V_L(t) \leq 1 \text{ km/h} \\ \frac{S(t)}{V_F(t) - V_L(t)}, & \text{otherwise} \end{cases} \quad (2)$$

The modified TTC proposed in this study was derived under the assumption that the speed difference between following and preceding vehicles is 1 km/h if it is less than 1 km/h. This modification enabled us to perform a continuous comparison with the relative speed data during the observation time, as the modified TTC yielded positive values even when $V_F(t) < V_L(t)$. Additionally, the modified TTC overcomes the limitation of overestimation in cases where the relative speed is less than 1 km/h by substituting $V_F(t) - V_L(t) = 1 \text{ km/h}$. These advantages enable the modified TTC to provide a continuous and realistic assessment of collision risk in car-following situations.

Figure 4 shows the TTC and modified TTC values calculated in 0.2 s intervals over a 12 s period. TTC underestimated the collision risk during the 0–1 s and 8–9 s periods owing to a decrease in relative speed and produced negative values when the preceding vehicle was faster than the following vehicle in the 1–6 s period. Conversely, the modified TTC generated positive values corresponding to the gap size between the two vehicles. These findings demonstrate that the modified TTC is more appropriate than the original TTC for use in continuous car-following situations. However, the modified TTC still has limitations, as it tends to distort collision risk by assuming constant $V_F(t) - V_L(t) = 1$ km/h when the speed difference between following and preceding vehicles is less than 1 km/h. To address this limitation, this study employed spectral analysis to estimate collision risk in a more robust manner, independently of traffic conditions.

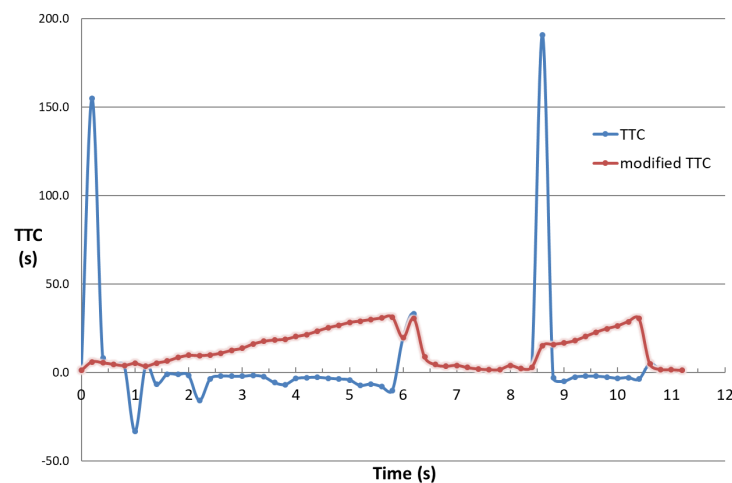


Figure 4. Comparison of TTC and modified TTC.

4.2. Step 2: Calculation of PSD

Fourier [25] discovered that all periodic waves can be decomposed into a series of subordinate waves called harmonics, and each harmonic contains unique wave characteristics that can be analyzed with spectral analysis, which is a methodology for analyzing the energy distribution of a spectrum of frequencies. There are two main methods for spectral analysis: the Fourier series, which breaks down a periodic wave function into harmonics, and the Fourier transform, which converts a wave function from the time domain to the frequency domain. Spectral analysis is well-suited for analyzing the relative speed waves in car-following situations because it can separate waves into harmonics and analyze the energies of each component, including collision risk.

The discrete Fourier transform is applied to transform a sequence of N complex numbers into another sequence of complex numbers (i.e., harmonics). If we define the aperiodic relative speed function observed in a particular time interval as $f(n)$, we can calculate the discrete Fourier transform $F[k]$ of $f(n)$ using Equation (3).

$$F[k] = \sum_{n=0}^{N-1} f(n)e^{-i2\pi k \frac{n}{N}} \quad (3)$$

The function $f(n)$ represents the relative speed observed at the n ($n = 0, 1, 2, \dots, N - 1$)-th time point in a particular time interval. Therefore, $F[k]$ represents the contribution rate of the k^{th} ($k = 0, 1, 2, \dots, N - 1$) harmonic of the relative speed wave frequency. The energy distribution of the harmonics is represented by $|F[k]|^2$ and is commonly used for comparison because $F[k]$ contains complex numbers and is not suitable for direct comparison. Assuming

that the cycle of $F[k]$ is infinite, $P[k]$ represents the PSD per unit frequency and can be calculated by dividing $|F[k]|^2$ by T .

$$P[k] = \lim_{T \rightarrow \infty} \left[\frac{1}{T} |F[k]|^2 \right] = \lim_{T \rightarrow \infty} \left[\frac{1}{T} F[k] F^*[k] \right] \quad (4)$$

where $F^*[k]$ is the conjugate spectrum of $F[k]$ and is calculated as follows:

$$F^*[k] = \sum_{n=0}^{N-1} f(n) e^{-i2\pi k(-\frac{n}{N})} = \sum_{n=0}^{N-1} f(n) e^{i2\pi k \frac{n}{N}} \quad (5)$$

Equation (4) can be transformed into a discrete form as follows:

$$P[k] = \lim_{T \rightarrow \infty} \left[\frac{1}{T} F[k] F^*[k] \right] \approx \frac{F[k] F^*[k]}{N} \quad (6)$$

$P[k]$, calculated using Equation (6), represents the energy density of the individual harmonics in the frequency spectrum of the relative speed data. A high value of $P[k]$ indicates that the corresponding harmonic significantly contributes to the overall change in relative speed. Therefore, $P[k]$ can be used to identify the most important frequency components for analyzing and understanding the dynamics of the car-following process.

Figure 5 shows a comparison of the PSD of the relative speed data in safe and risky car-following situations using spectral analysis. The safe situation showed a low PSD value and a small range of frequency, indicating a similar scale of reaction to the stimulus and a small variation in relative speed. In contrast, the risky situation showed a larger PSD value and a wider range of frequencies, indicating an amplified reaction to the stimulus and a larger variation in relative speed caused by abrupt acceleration and deceleration. However, both situations showed that the PSD was mostly concentrated at frequencies less than 0.05 Hz, indicating that long-period components or smooth variations in relative speed were prevalent.

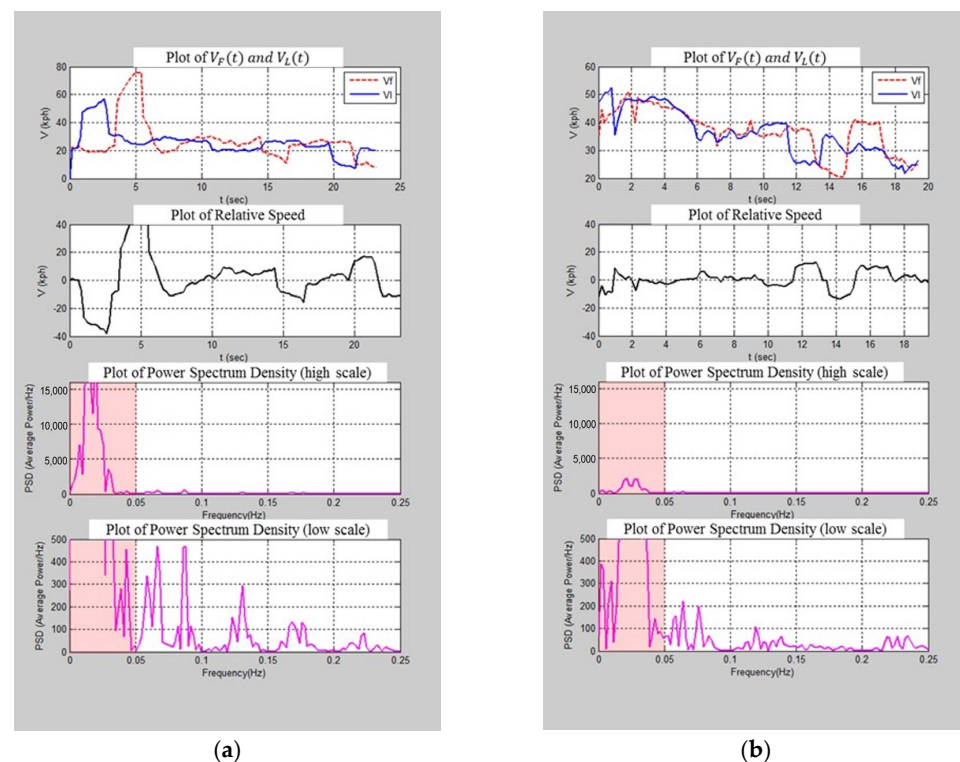


Figure 5. Comparison of PSD: (a) safe car-following situation and (b) risky car-following situation.

For a more detailed analysis, the maximum PSD values on the y-axis were reduced from 15,000 to 500 Hz. This reduction in the PSD scale magnified the medium-value PSD distributed over the frequency region above 0.05 Hz. In safe driving situations, the PSD of the relative speed was dominated by low-frequency components. As the frequency increased, PSD significantly decreased.

4.3. Step 3: Correlation Analysis between Modified TTC and PSD

We conducted a correlation analysis between the modified TTC and PSD, $P[k]$, to identify the frequency bands of the harmonics that exhibited a statistically significant correlation with the modified TTC. The modified TTC was calculated as the average over a time window of 15 s on the 170 datasets. If specific bands of harmonics are found to be correlated with the risky driving of a following vehicle, their $P[k]$ values are also correlated with the collision probability. Thus, it is possible to detect risky driving behaviors of a following vehicle by performing a correlation analysis between the $P[k]$ values and the modified TTC. If there is a significant correlation between the specific frequency bands of the PSD and the modified TTC, the frequency bands can be utilized to calculate a surrogate measure for the collision risk of the following vehicle, which overcomes the limitations of the modified TTC mentioned earlier. The sum and ratios of the PSD values were calculated according to the frequency components and used in the correlation analysis. In this study, both the sum and ratio of the PSD were calculated in two ranges divided by the frequency value (0.05 Hz).

The high frequency of oscillations in the relative speed data caused by frequent changes in speed of the following or preceding vehicle resulted in a large sum of PSD values. As the collision risk of both vehicles increased and the modified TTC decreased, the sum of the PSD values for both frequency ranges increased, as shown in Figure 6a,b. However, the PSD ratio showed a different correlation with the modified TTC depending on the frequency range. Specifically, Figures 3d and 6c show that the ratio of the PSD decreased at frequencies below 0.05 Hz, whereas it increased at frequencies above 0.05 Hz, as the modified TTC decreased and the collision risk increased. The correlation analysis between the PSD ratio and the modified TTC presented in Table 1 shows that the frequency components ranging from 0 to 0.05 Hz had a positive correlation with the modified TTC. When the frequency range was segmented into 0.025 Hz ($\frac{1}{2}$ of 0.05 Hz) and 0.0167 Hz ($\frac{1}{3}$ of 0.05 Hz), the correlation coefficient in the 0–0.017 Hz range had the highest value (0.312), whereas negative correlation coefficients were observed in the other frequency bands. This positive correlation indicates that as the modified TTC increases, the energy density low-frequency components increase, suggesting lower collision risk. The negative correlation coefficients in the other frequency bands indicate that modified TTC would be decreased as these energy density frequency components increase.

The p -value for all three frequency ranges was 0.000. The results of the correlation analysis suggest that the frequency components below 0.05 Hz, particularly in the range of 0–0.017 Hz, have a significant positive correlation with the modified TTC. The collision risk decreased when the ratio of the PSD frequency components in the range of 0–0.017 Hz increased. This indicates that low-frequency components, which represent long-period changes in relative speed, are inversely proportional to collision risk, unlike high-frequency components, which represent short-period fluctuations in relative speed. These findings suggest that the low-frequency components of PSD can be used as a surrogate measure of collision risk in car-following situations.

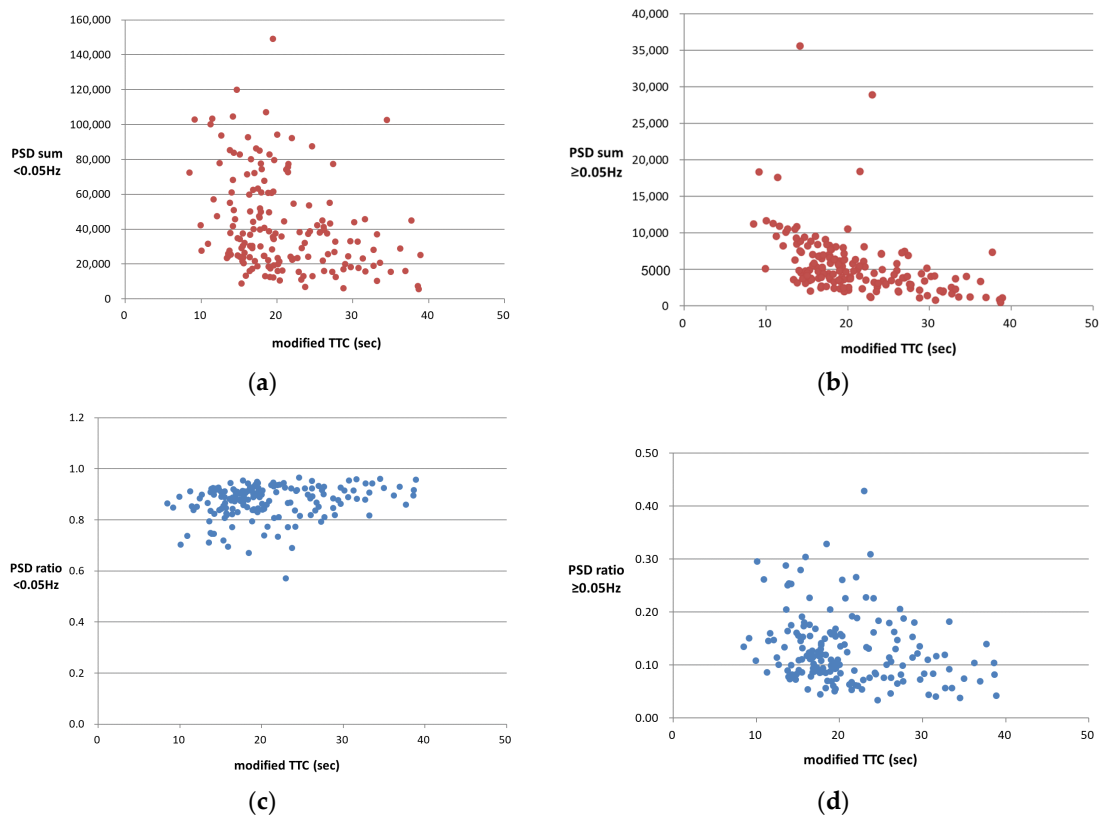


Figure 6. Correlation analysis between the modified TTC and PSD: (a) sum of PSD values at frequencies below 0.05 Hz, (b) sum of PSD values at frequencies above 0.05 Hz, (c) ratio of PSD at frequencies below 0.05 Hz, and (d) ratio of PSD at frequencies above 0.05 Hz.

Table 1. Correlation analysis of the segmented frequency ranges.

0.05 Hz Interval			0.025 Hz Interval			0.0167 Hz Interval		
Frequency (Hz)	Correlation Coefficient	<i>p</i> -Value	Frequency (Hz)	Correlation Coefficient	<i>p</i> -Value	Frequency (Hz)	Correlation Coefficient	<i>p</i> -Value
0–0.05	0.290	0.000	0–0.025	0.291	0.000	0–0.017	0.312	0.000
			0.025–0.050	−0.232	0.002	0.017–0.033	−0.189	0.013
						0.033–0.050	−0.195	0.011
0.05–0.10	−0.264	0.001	0.050–0.075	−0.270	0.000	0.050–0.067	−0.239	0.002
			0.075–0.100	−0.099	0.201	0.067–0.083	−0.155	0.044
						0.083–0.100	−0.161	0.036
0.10–0.15	−0.213	0.005	0.100–0.125	−0.206	0.007	0.100–0.117	−0.208	0.006
			0.125–0.150	−0.151	0.049	0.117–0.133	−0.176	0.021
						0.133–0.150	−0.105	0.175
0.15–0.20	−0.175	0.023	0.150–0.175	−0.162	0.035	0.150–0.167	−0.159	0.038
			0.175–0.200	−0.155	0.044	0.167–0.183	−0.147	0.055
						0.183–0.200	−0.113	0.141
0.20–0.25	−0.221	0.004	0.200–0.225	−0.257	0.001	0.200–0.217	−0.192	0.012
			0.225–0.250	−0.139	0.070	0.217–0.233	−0.217	0.004
						0.233–0.250	−0.122	0.112

4.4. Step 4: Development of Driving-Pattern Indices

To assess the driving patterns of following vehicles, we calculated three indices from the vehicle trajectory data in a car-following situation: reaction time, stimulus compliance index, and collision-risk aversion index (CRAI).

Reaction time and stimulus compliance index are determined with the cross-correlation of the speed data of preceding and following vehicles. Let (X_t, Y_t) represent a pair of preceding and following vehicles' speed values. The cross-correlation function and coefficient are given by Equations (7) and (8), respectively.

$$C_{XY}(\tau) = E[X_{t-\tau}Y_t] \quad (7)$$

$$R_{XY}(\tau) = \frac{C_{XY}(\tau)}{\sigma_X(t-\tau)\sigma_Y(t)} \quad (8)$$

where τ is the time delay between two speed values; $X_{t-\tau}$ is the speed of the leading vehicle at time $t - \tau$; Y_t is the speed of the following vehicle at time t ; $C_{XY}(\tau)$ is the cross-correlation function between $X_{t-\tau}$ and Y_t ; and $R_{XY}(\tau)$ is the cross-correlation coefficient.

In a car-following situation, the following vehicle follows the preceding vehicle at appropriate gap, speed, and acceleration. If the preceding vehicle accelerates or decelerates, the following vehicle adapts its speed with a certain time delay to reach the desired speed or safely proceed behind it. The reaction time is determined by the time delay that maximizes the cross-correlation coefficient and overlapping area of the two speed data. The reaction time is an indicator of how quickly the following vehicle responds to changes in speed of the preceding vehicle.

The cross-correlation coefficient is calculated using the time delay. If the cross-correlation coefficient is close to 1, then the following vehicle is more likely to conform to the stimulus of the preceding vehicle. If the cross-correlation coefficient is close to zero or has a negative value, the following vehicle is more likely to travel independently of the preceding vehicle. The stimulus compliance index is determined using the cross-correlation coefficient and reaction time τ . This is an indicator of how well the following vehicle conforms to the change in speed of the preceding vehicle. A higher stimulus compliance index indicates better tracking of the speed of the preceding vehicle.

In Figure 7, the distribution of the stimulus compliance index is skewed toward 1, indicating that most following vehicles tend to conform to the speed changes of preceding vehicles in car-following situations. The reaction time ranged from 0.80 to 4.20 s, with an average of 2.09 s, which is consistent with the assumption in most car-following models. The reaction time of 4.20 s was observed when the average distance headway was approximately 21.6 m, whereas the reaction time of 0.80 s was observed when the average distance headway was approximately 11.1 m.

The similarity in magnitude between stimulus and response is indicated by the stimulus compliance index. The CRAI represents the extent to which the following vehicle tends to avoid collision risk. It is calculated by dividing the sum of the PSD frequency components showing low collision risk by the total sum of the PSD values. In this study, the frequency range of 0–0.017 Hz was identified as the range with low collision risk. Therefore, the CRAI was calculated by dividing the sum of the PSD values in this frequency range by the total sum of the PSD values, as shown in Equation (9). A high CRAI value indicates that the following vehicle is more likely to maintain a safe distance from the preceding vehicle and avoid sudden acceleration and deceleration in response to the speed of the preceding vehicle, thereby reducing the risk of collision.

$$\text{Collision – Risk Aversion Index (CRAI)} = \frac{\text{PSD of harmonics} < 0.017 \text{ Hz}}{\text{Total PSD}} \quad (9)$$

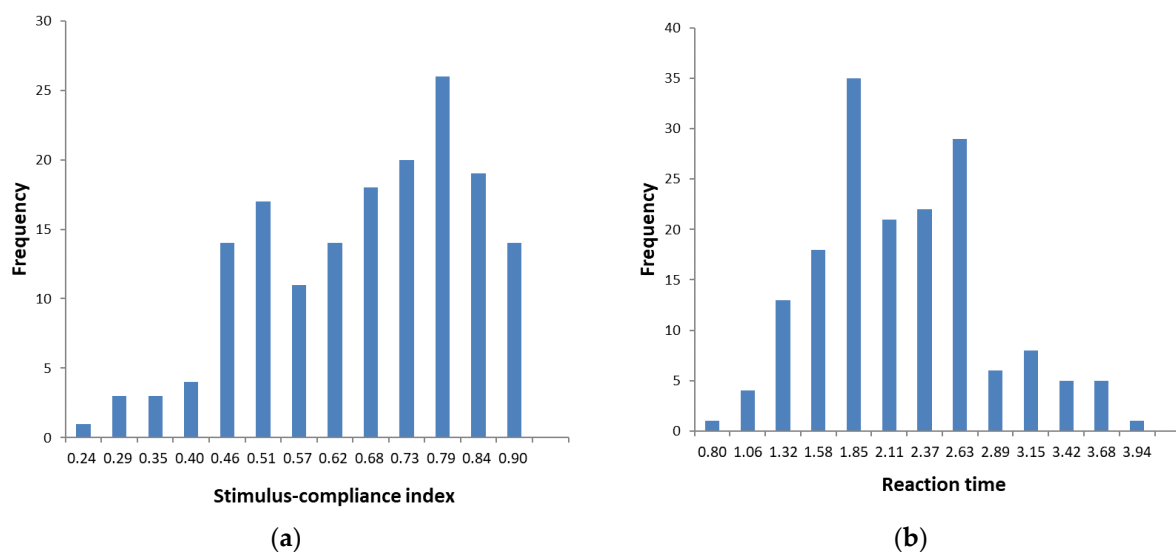


Figure 7. Histograms: (a) stimulus compliance index and (b) reaction time.

5. Validation and Discussion

A correlation analysis was conducted to validate the CRAI of following vehicles by examining the correlation between the PSD ratio and the modified TTC using additional relative speed datasets. A total of 140 relative speed datasets collected from 27 May 2010 to 1 June 2010 at the same study site were used for this validation. The findings from the correlation analysis presented in Table 2 are consistent with those presented in Table 1, demonstrating a positive correlation coefficient in the frequency range below 0.017 Hz and negative correlation coefficients in the frequency ranges above 0.017 Hz. These results further support the validity of the CRAI calculation by dividing the sum of the PSD values below 0.017 Hz by the total sum of the PSD values.

Table 2. Validation of CRAI of following vehicles.

Frequency (Hz)	Initial Analysis Results		Verification Analysis Results	
	Correlation Coefficient	<i>p</i> -Value	Correlation Coefficient	<i>p</i> -Value
0–0.017	0.312	0.000	0.409	0.000
0.017–0.033	−0.189	0.013	−0.341	0.000
0.033–0.050	−0.195	0.011	−0.313	0.000
0.050–0.067	−0.239	0.002	−0.158	0.063
0.067–0.083	−0.155	0.044	−0.229	0.006
0.083–0.100	−0.161	0.036	−0.171	0.044
0.100–0.117	−0.208	0.006	−0.193	0.023
0.117–0.133	−0.176	0.021	−0.229	0.006
0.133–0.150	−0.105	0.175	−0.128	0.133
0.150–0.167	−0.159	0.038	−0.154	0.069
0.167–0.183	−0.147	0.055	−0.300	0.000
0.183–0.200	−0.113	0.141	−0.149	0.078
0.200–0.217	−0.192	0.012	−0.134	0.133
0.217–0.233	−0.217	0.004	−0.230	0.006
0.233–0.250	−0.122	0.112	−0.144	0.089

To assess the applicability of the CRAI to real-world car-following situations, we compared the index with other traffic variables, such as average travel speed, average relative speed, and space headway. Table 3 presents the results of the study. Our analysis found that the CRAI did not demonstrate a significant relationship with the average travel speed. However, a clear correlation was observed between the index and average relative speed (i.e., speed of the following vehicle – speed of the preceding vehicle). Specifically, following vehicles with lower index values (i.e., more aggressive drivers) tended to exhibit higher average relative speed and smaller space headway, which aligns with actual traffic accident scenarios. The proposed CRAI can be particularly useful for AVs in assessing the tendency of following vehicles to engage in collision risk. By utilizing this index, AVs can plan safer driving strategies, such as selecting appropriate car-following speed and optimal gaps during lane-changing maneuvers.

Table 3. Comparison of CRAI with traffic variables.

CRAI	Frequency	Average Travel Speed (km/h)	Average Relative Speed (km/h)	Space Headway (m)
<0.1	3	38.18	0.37	9.33
0.1–0.2	8	56.94	−0.14	12.72
0.2–0.3	16	41.66	−0.12	11.02
0.3–0.4	36	39.86	−0.32	13.09
0.4–0.5	44	39.99	−0.68	15.12
0.5–0.6	40	40.31	−0.82	16.24
0.6–0.7	17	35.66	−1.25	17.70
0.7–0.8	6	40.06	−0.79	36.23
0.8–1	0	-	-	-

To demonstrate the efficacy of the CRAI developed in this study, two sets of preceding and following vehicles' trajectory data are presented in Figure 8, representing high- and low-CRAI scenarios. The reaction time, stimulus compliance index, and other traffic variables were consistent between the two sets. However, for the trajectory with a low CRAI value (0.078), three risky situations occurred when the spatial headway was less than 1 m. During the observation interval, abrupt changes occurred in the space headway, and the following vehicle appeared to incur collision risk. Conversely, in the trajectory with a high CRAI value (0.531), the space headway remained constant at approximately 10 m, that is, there were minimal changes in space headway. These results highlight the CRAI as a valuable metric for identifying the driving pattern of a following vehicle.

Based on the analysis of car-following situations, the relationship between driving-pattern indices and traffic variables was identified. This relationship is more apparent in risky car-following situations, as shown in Figure 9. Despite the increase in speed of the two vehicles in a car-following relationship, if the reaction time of the following vehicle decreases and it reacts quickly, the risk of collision is reduced, with no significant changes in the stimulus compliance index and CRAI. However, an increase in the average relative speed leads to a decrease in both the reaction time of the following vehicle and the collision-aversion index, along with an increase in the stimulus compliance index. A decrease in the average headway corresponds to a decrease in both reaction time and the CRAI, with no significant change in the stimulus compliance index. These findings suggest that in risky car-following situations, following vehicles tend to exhibit higher sensitivity and aggressiveness, which is consistent with the results of existing research on traffic behaviors.

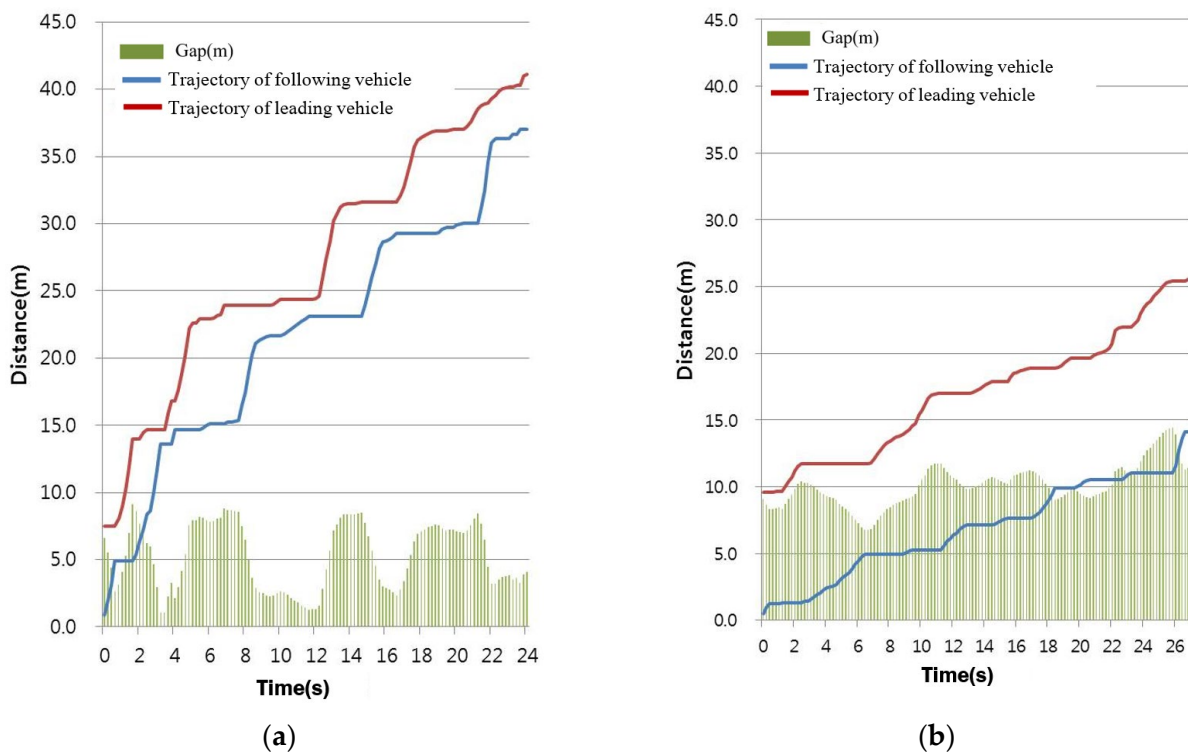


Figure 8. Vehicle trajectory: (a) low CRAI (0.078) and (b) high CRAI (0.531).

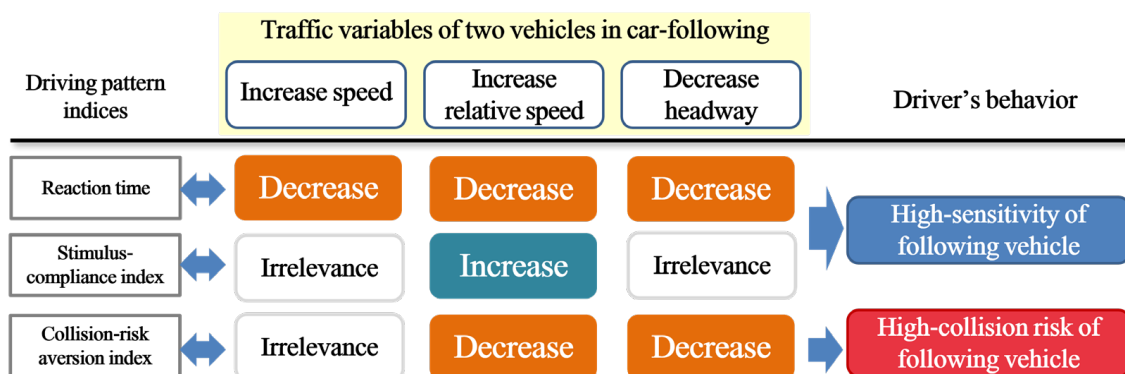


Figure 9. Relationship between driving-pattern indices and traffic variables in risky car-following situation.

6. Conclusions

The purpose of this study was to develop a methodology to analyze the driving risk of a following vehicle in order to reduce the risk of rear-end collision for AVs. An analysis method using spectral analysis is suggested based on the fact that the relative speed of two vehicles in a car-following situation shows as a waveform. First, the relative speed waves of two vehicles in a following relationship were decomposed into individual harmonics with the discrete Fourier transform methodology. Then, with a correlation analysis between the energy density of harmonics using frequency and the modified TTC, it was found that the PSD of 0.017 Hz or less showed a high correlation, and this was defined as the CRAI. In addition, reaction time and the stimulus compliance index were developed as driving-pattern indices that can calculate the risk of collision between two vehicles in a following relationship.

The contributions of this study are twofold: First, we propose a robust spectral analysis-based technique for identifying the relationship between driving patterns and collision risk, which can be used in all traffic scenarios. This relationship can be further utilized to develop more effective methods for preventing rear-end collisions and improving traffic

safety. Second, we propose a process to compute three indices—reaction time, stimulus compliance index, and CRAI—to describe the driving pattern of following vehicles. The behavior of risky drivers in car-following situations can be described well by these indices, which are consistent with the results of existing research. The results of this study can be applied to control and judgment algorithms for AVs. First, reaction time and the stimulus compliance index of surrounding vehicles can be calculated using the information collected with sensors mounted on AVs. Utilizing these indices, AVs can make safe path planning like planning lane changes and turns. Additionally, by utilizing the CRAI, AVs can control speed and distance to prevent collisions with vehicles located in front of and behind them. The indices can be applied to ADASs as well as AVs to improve driving convenience and support safe driving for CVs.

However, our proposed approach has limitations in field applications. The CRAI was developed for car-following situations; however, collision risk must be considered in various situations besides car following, such as lane changing, merging, and weaving. Additionally, an extensive analysis of the threshold values of the index and a performance comparison with existing car-following models are suggested for future research.

Author Contributions: Data collection, Y.K.; Methodology and Analysis, C.C.; Writing—original draft, C.C.; Writing—review and editing, Y.K. All authors have read and agreed to the published version of the manuscript.

Funding: This work was supported by a Korea Agency for Infrastructure Technology Advancement (KAIA) grant funded by the Ministry of Land, Infrastructure, and Transport (grant RS-2022-00141102), and the authors are grateful to KAIA for economic supports.

Institutional Review Board Statement: Not applicable.

Informed Consent Statement: Not applicable.

Data Availability Statement: The data used to support the findings of this study are available upon request from the corresponding author.

Conflicts of Interest: The authors declare no conflict of interest.

References

1. National Highway Traffic Safety Administration (NHTSA). *Traffic Safety Facts: 2019 Data*; U.S. Department of Transportation: Washington, DC, USA, 2020. Available online: <https://crashstats.nhtsa.dot.gov/Api/Public/ViewPublication/813010> (accessed on 7 February 2023).
2. Tak, S.; Kim, S.; Lee, D.; Yeo, H. A comparison analysis for surrogate safety measures with car-following perspectives for advanced driver assistance system. *J. Adv. Transp.* **2018**, *2018*, 8040815. [CrossRef]
3. Muzahid, A.J.M.; Kamarulzaman, S.F.; Rahman, M.A.; Murad, S.A.; Kamal, M.A.S.; Alenezi, A.H. Multiple vehicle cooperation and collision avoidance in automated vehicles: Survey and an AI-enabled conceptual framework. *Sci. Rep.* **2023**, *13*, 603. [CrossRef] [PubMed]
4. Cabrera, A.; Goyal, S.; Martinoli, A. A new collision warning system for lead vehicles in rear-end collisions. In Proceedings of the IEEE Intelligent Vehicles Symposium, Madrid, Spain, 3–7 June 2012; pp. 674–679. [CrossRef]
5. Wang, C.; Wie, Y.; Huang, H.; Liu, P. A review of surrogate safety measures and their applications in connected and automated vehicles safety modeling. *Accid. Anal. Prev.* **2021**, *157*, 106157. [CrossRef] [PubMed]
6. Bretti, G.; Natalini, R.; Piccoli, B. A fluid-dynamic traffic model on road networks. *Arch. Comput. Methods Eng.* **2007**, *14*, 139–172. [CrossRef]
7. Maerivoet, S.; De Moor, B. Cellular automata models of road traffic. *Phys. Rep.* **2005**, *419*, 1–64. [CrossRef]
8. Pariota, L.; Bifulco, G.N.; Brackstone, M. A linear dynamic model for driving behavior in car following. *Transp. Sci.* **2016**, *20*, 1032–1042. [CrossRef]
9. Kim, Y. Online Traffic Flow Model Applying the Dynamic Flow-Density Relation. Ph.D. Dissertation, Technical University of Munich, Munich, Germany, 2002.
10. Treiber, M.; Kesting, A. *Traffic Flow Dynamics: Data, Models*; Springer: Berlin/Heidelberg, Germany, 2013; ISBN 978-3-642-32459-8.
11. Reuschel, A. Fahrzeugbewegungen in der Kolonne. *Osterreichisches Ing. Arch.* **1950**, *4*, 193–215.
12. Pipes, L.A. An operational analysis of traffic dynamics. *J. Appl. Phys.* **1953**, *24*, 274–281. [CrossRef]
13. Gazis, D.C.; Herman, R.; Rothery, R.W. Nonlinear follow-the-leader models of traffic flow. *Oper. Res.* **1961**, *9*, 545–567. [CrossRef]
14. Gipps, P.G. A behavioural car-following model for computer simulation. *Transp. Res. Part B* **1981**, *15*, 105–111. [CrossRef]

15. Helly, W. Simulation of bottlenecks in single-lane traffic flow. In Proceedings of the Symposium on Theory of Traffic Flow, Detroit, MI, USA, 7–8 December 1959; pp. 207–238.
16. Zhou, Y.; Ahn, S. Robust local and string stability for a decentralized car following control strategy for connected automated vehicles. *Transp. Res. Part B Methodol.* **2019**, *125*, 175–196. [[CrossRef](#)]
17. Kontar, W.; Li, T.; Srivastava, A.; Zhou, Y.; Chen, D.; Ahn, S. On multi-class automated vehicles: Car-following behavior and its implications for traffic dynamics. *Transp. Res. Part C Emerg. Technol.* **2021**, *128*, 103166. [[CrossRef](#)]
18. Zou, Y.; Zhu, T.; Xie, Y.; Zhang, Y.; Zhang, Y. Multivariate analysis of car-following behavior data using a coupled hidden Markov model. *Transp. Res. Part C Emerg. Technol.* **2022**, *144*, 103914. [[CrossRef](#)]
19. Colmenares, J.A.R.; Uriarte, E.A.; del Campo, I. Driving-Style Assessment from a Motion Sickness Perspective Based on Machine Learning Techniques. *Appl. Sci.* **2023**, *13*, 1510. [[CrossRef](#)]
20. Du, Y.; Chen, J.; Zhao, C.; Liu, C.; Liao, F.; Chan, C.Y. Comfortable and energy-efficient speed control of autonomous vehicles on rough pavements using deep reinforcement learning. *Transp. Res. Part C Emerg. Technol.* **2022**, *134*, 103489. [[CrossRef](#)]
21. Hayward, J.C. Near-miss determination through use of a scale of danger. *Highw. Res. Rec.* **1972**, *384*, 24–34.
22. Mahmud, S.M.S.; Ferreira, L.; Hoque, M.S.; Tavassoli, A. Application of proximal surrogate indicators for safety evaluation: A review of recent developments and research needs. *IATSS Res.* **2017**, *41*, 153–163. [[CrossRef](#)]
23. Barış, M. Hourly significant wave height prediction via singular spectrum analysis and wavelet transform based models. *Ocean Eng.* **2023**, *281*, 114771.
24. Wang, Y.; Bao, S.; Du, W.; Ye, Z.; Sayer, J.R. A spectral power analysis of driving behavior changes during the transition from nondistracted to distracted. *Traffic Inj. Prev.* **2017**, *18*, 826–831. [[CrossRef](#)] [[PubMed](#)]
25. Fourier, J. *The Analytical Theory of Heat*; Cambridge University Press: Cambridge, UK, 1878; pp. 168–209.

Disclaimer/Publisher’s Note: The statements, opinions and data contained in all publications are solely those of the individual author(s) and contributor(s) and not of MDPI and/or the editor(s). MDPI and/or the editor(s) disclaim responsibility for any injury to people or property resulting from any ideas, methods, instructions or products referred to in the content.